Molecular Modeling of Structure Development upon Quenching of a Polymer Solution

Yves Termonia

Central Research and Development, Experimental Station, E. I. du Pont de Nemours, Inc., Wilmington, Delaware 19880-0356

Received April 23, 1997; Revised Manuscript Received June 23, 1997[⊗]

ABSTRACT: We simulate on the computer the kinetics of structure formation upon quenching a polymer solution inside a two-phase region. Our description is on a mesoscopic scale, and the polymer is represented by a chain of beads on a cubic lattice. The results presented are for a 10% solution of polyethylene with a monodisperse molecular weight $M = 140\,000$. We find that the polymer structure grows in two stages. In the first stage, a bicontinuous percolated microstructure is formed through spinodal decomposition and the sizes of the phase domains increase linearly with time. Within that stage, deep quenches lead to lacy structures made of fine and dense fibrils, whereas shallow quenches form wide ribbons with many voids. At the percolation-to-cluster transition, a second stage occurs in which the polymer network breaks into isolated aggregates by diffusive coarsening and sizes grow more slowly as $R^4 \sim Kt$.

1. Introduction

The quenching of a polymer solution induced by a sudden change in temperature, pressure, or solution composition is widely used in a variety of polymer-manufacturing processes including membrane formation,[1] fiber spinning,[2] and colloidal aggregation,[3] to mention only a few. All these applications deeply rely on a basic understanding of the factors controlling the development of morphology of the precipitated polymer. Recently,[4] we presented a model study of the coagulation of a polymer solution brought upon by *diffusion* of a nonsolvent. In the present paper, we focus on the faster process of phase separation inside a binary polymer/solvent system caused by an abrupt change in external temperature and/or pressure. That problem is of great importance in polymer-processing techniques based on thermally-induced phase separation (TIPS)[5] or on rapid expansion of supercritical solutions (RESS).[6] A typical example of the latter is the flash spinning process in which a heated polymer solution under high pressure is rapidly released through a spinnerette, leading to the formation of a fibrillar polymeric network.

A review of the existing literature reveals that the equilibrium properties of polymers in dilute solutions are reasonably well understood.[7] Polymer−solvent phase equilibria can be easily obtained through the use of the classical Flory−Huggins mean-field lattice model[8] or from more recent computer simulations of Gibbs ensembles.[9−10] Our understanding of the development of polymer morphology inside the coexistence curve is, however, much less satisfactory, and all previous investigations have been restricted to kinetic model studies of the collapse of a *single* polymer chain.[11−13] In the present work, we turn to multichain systems and we focus on the very early stages ($t \ll 1$ s) of spinodal decomposition, during which equilibrium concentrations are being established. We are particularly interested in the dependence of the early polymer structure on molecular weight, polymer concentration, and quenching conditions.

For simplicity, our study is for a polymer system with a monodisperse molecular weight ($M = 140\,000$) and a model solvent leading to a phase diagram with an upper critical solution temperature (UCST). It is also important to note that our description is on a mesoscopic scale and the polymer is represented by a chain of beads on a cubic lattice. Future work will be directed toward a detailed study of the importance of the molecular weight distribution and of the shape of the polymer−solvent coexistence curve.

2. Model

All our simulations have been performed on a simple cubic lattice (coordination number $\kappa = 6$) of up to $90 \times 90 \times 90$ sites with periodic boundary conditions. The unit lattice length is set equal to the statistical segment length, l, of the polymeric chains.

We start by generating the state of the polymer solution at infinite temperature. This is realized as follows. An ordered array of chains is first constructed on the lattice for a given value of the chain volume fraction, V_f, and chain length, N (henceforth in statistical segment units). That array is then randomized by a series of Monte Carlo moves of two kinds. The first is a nonlocal reptation which randomly moves a bond from one end of a chain to the other.[12] The second incorporates local random moves such as end-flip, two-bond kink jump, and three-bond crankshaft motion.[14]

After complete randomization of the chains, which is usually obtained after $10N$ moves per bond, the polymer network is quenched to a (reduced) temperature $-k_BT/\epsilon$ in which $\epsilon < 0$ denotes the interaction energy between pairs of nonbonded nearest-neighbor chain segments. The new configurations of the chains are then obtained, as a function of time, by using the *local* Monte Carlo moves described above (i.e., nonlocal reptation is excluded) which are made to occur at a rate[4]

$$\nu = \tau^{-1} \exp[-(U_f - U_i)/k_BT] \qquad (1)$$

in which U_f and U_i denote the local energy in the final and initial states, respectively. In eq 1, τ corresponds to the reorientation time of a statistical segment, which is of the order of 10^{-8} s.[11] After each attempted move, the overall time t is incremented by $1/[\nu_{max}n]$, in which ν_{max} represents the highest rate among all n possible moves on the lattice.[4]

The results, to be presented below, are for application to polyethylene. For that polymer, the length of a statistical segment is $l \sim 10$ Å.[15] The largest chain length is set equal to $N = 10^3$ statistical segments, which corresponds to a molecular weight of 140 000g.[15]

[⊗] Abstract published in *Advance ACS Abstracts,* August 15, 1997.

S0024-9297(97)00565-2 CCC: $14.00

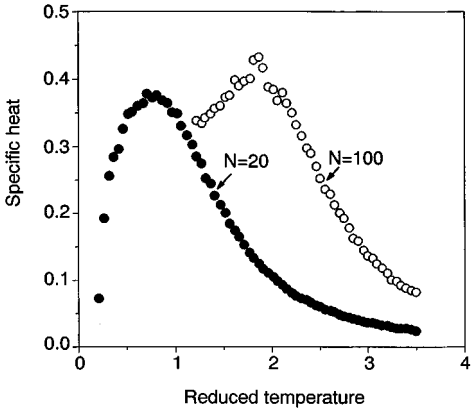

Figure 1. Dependence of the specific heat (eq 2) on reduced temperature $-k_BT/\epsilon$ for single chains of length $N = 20$ and 100. Each data point corresponds to 2×10^7 Monte Carlo moves.

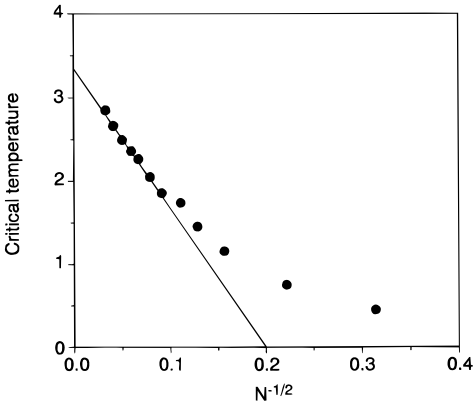

Figure 2. Dependence of the critical temperature $-k_BT_c/\epsilon$ on $N^{-1/2}$ for single chains.

3. Results and Discussion

(3a) Phase Equilibria. Since we are, in the present section, mainly interested in static equilibrium configurations, both local and nonlocal (i.e., reptation) moves have been used in the Monte Carlo simulations. In order to study phase equilibria, we compute the specific heat[16]

$$C = [\langle \eta^2 \rangle - \langle \eta \rangle^2]\epsilon^2/[(N+1)k_BT^2] \qquad (2)$$

in which η denotes the number of nearest-neighbor nonbonded polymer segments. Figure 1 shows the calculated dependence of C on the reduced temperature ($-k_BT/\epsilon$) for single chains of length $N = 20$ and 100. For each temperature, up to 2×10^7 Monte Carlo moves were performed. The figure clearly reveals a maximum near critical temperatures $-k_BT_c/\epsilon = 0.85$ and 1.85, which correspond to the coil-to-globule collapse transition of the chains. Figure 2 shows that the dependence of $-k_BT_c/\epsilon$ on $N^{-1/2}$ for single chains is linear at large N, in agreement with previous simulation results.[16,17] Extrapolation to infinite chain lengths leads to a (reduced) θ temperature near 3.36, which agrees reasonably well with the values $T_\theta = 3.65$ predicted with the scanning simulation method[18] and $T_\theta = 3.25$ obtained from more recent molecular dynamics[19] and Monte Carlo[20] simulations

Simulation results for the dependence of $-k_BT_c/\epsilon$ on the polymer volume fraction, V_f, are presented in Figure 3 for chains of length $N = 20$ (symbol ○), 60 (□), and 1000 (△). Note the pronounced asymmetry of the curves and the shift of their maxima toward higher T_c and lower V_f with an increase in N, in perfect accordance with experiment.[21] Also represented are theoretical predictions obtained from two other approaches. Symbol ● denotes data obtained by Madden *et al.*[9] for $N = 100$, using a slab geometry in which the polymer-rich phase is condensed against an adhesive boundary. Data represented with the symbol ■ are from Mackie *et al.*[10] for $N = 64$, using Gibbs ensemble simulations based on the deletion and insertion of whole lattice layers. These data, originally obtained for a coordination number $\kappa = 26$, have been renormalized to our current $\kappa = 6$, also taking into account the fact that in the present work ϵ denotes the energy for *polymer−polymer* interactions. Inspection of Figure 3 shows that the data from Madden *et al.* and from Mackie *et al.* are, again, in good qualitative agreement with our model predictions. A similar agreement can be found with recent predictions from the configurational-bias-vaporization method.[22]

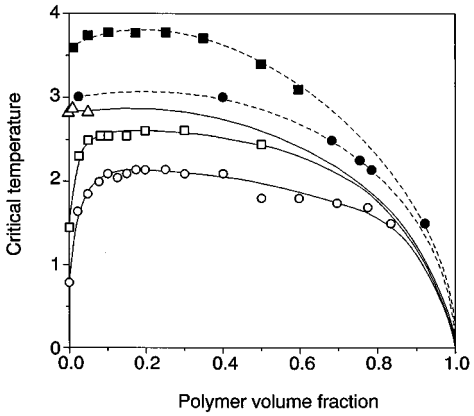

Figure 3. Dependence of the critical temperature $-k_BT_c/\epsilon$ on polymer volume fraction. Results obtained with the help of our approach are denoted by open symbols: (○) $N = 20$; (□) $N = 60$, and (△) $N = 1000$. Both local and nonlocal (i.e., reptation) moves have been used in our Monte Carlo simulations. Filled-in symbols are reproduced from ref 9 (●, $N = 100$) and ref 10 (■, $N = 64$). The curves are drawn to guide the eye.

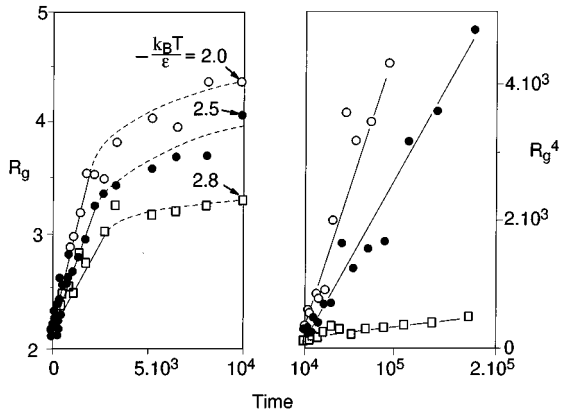

Figure 4. Time dependence of the average radius, R_g, of the largest spheres that can be drawn within the pure solvent domains. The figure is for different quenching temperatures. The time is in units of τ.

(3b) Development of Morphology upon Quenching. In the present section, we turn to a detailed study of the structure development upon quenching inside the binodal curves of Figure 3. Our analysis is for polymer chains of length $N = 10^3$ and volume fraction $V_f = 0.1$. All our computations have been performed on a SGI Power Challenge. A typical simulation, such as that presented in Figure 9 (case ii), takes approximately 70 h on a 100-MHz processor.

A convenient way of investigating the kinetics of polymer separation during spinodal decomposition (SD)

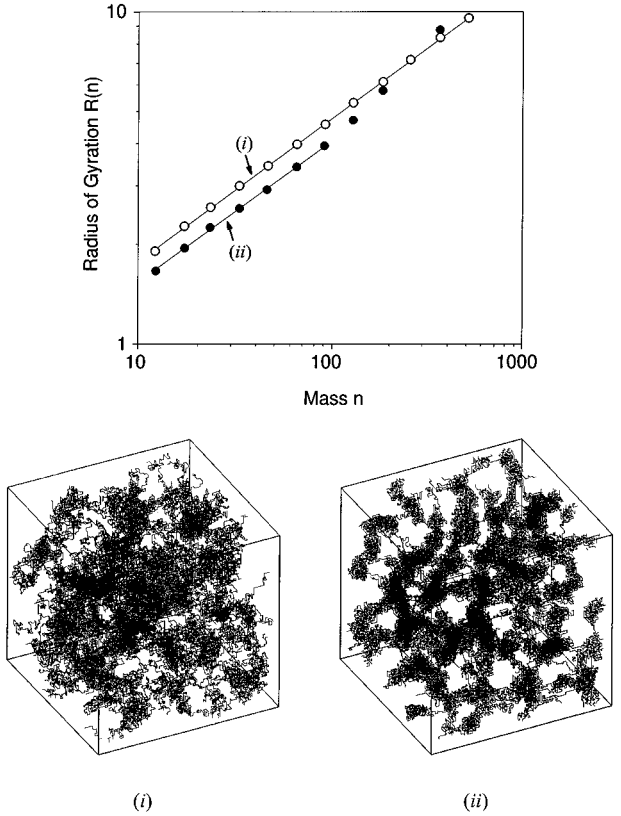

Figure 5. Early time structures. The figure is for a time $t = 5 \times 10^3\tau$ and quenching temperatures $-k_BT/\epsilon = 2.5$ (case i) and $-k_BT/\epsilon = 1.0$ (case ii). (a) Radius *vs* size dependence of clusters of polymer segments. (b) Polymer morphologies. The representations are for cubic lattices of 70 unit lengths (~70 nm) in each direction.

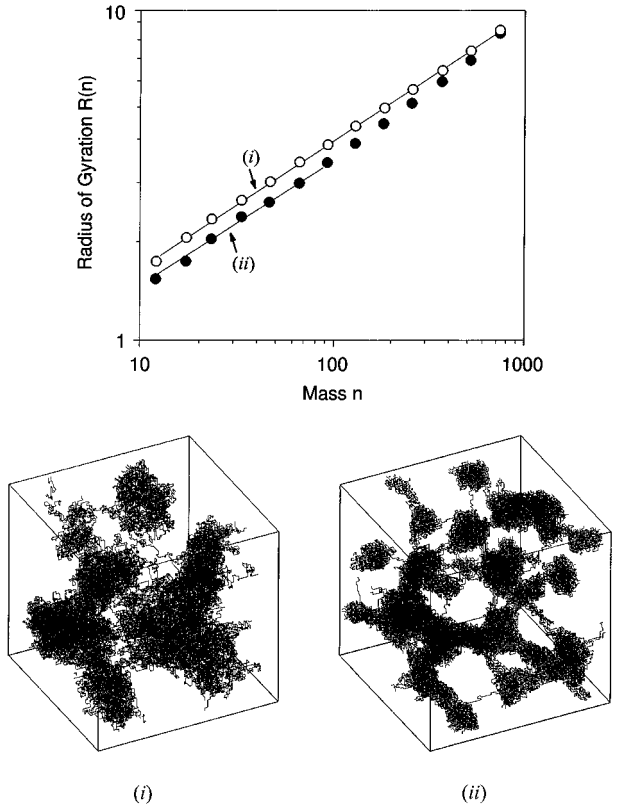

Figure 6. Late time structures. Same as Figure 5 but, for $t = 1.5 \times 10^5\tau$.

is through a study of the rate of growth of the pure solvent phase. The size of that phase is estimated by the average radius, R_g, of the largest spheres that can be drawn within the pure solvent domains.[23] Figure 4 shows the dependence of R_g on time for different quenching temperatures $-k_BT/\epsilon = 2.0$ (symbol ○), 2.5 (●), and 2.8 (□). We start by focusing on our model results for short times (left part of the figure). For $t < 5 \times 10^3\tau$, R_g is seen to grow linearly with time, which is indicative of a process driven by hydrodynamic interactions between segments on the same chain.[24, 25] This "nonclassical" regime has been observed experimentally in the early stages of SD in a polymer solution and attributed to the low polymer concentration where hydrodynamic interactions are not screened out.[26] Note that our model results also indicate a decrease in the rate of growth of R_g with an increase in quenching temperature T. A convenient way of studying polymer morphology within the early stages of the SD regime is through the dependence of the radius of gyration, R, on the mass, n, of arbitrary clusters of chain segments:[27−28]

$$[R(n)]^{d_f} \sim n \tag{3}$$

in which d_f defines a "fractal" dimension. Figure 5a shows the (log−log) dependence of $R(n)$ on n obtained at $t = 5 \times 10^3\tau$ for $-k_BT/\epsilon = 2.5$ (case i) and 1.0 (case ii). For small $n < 1000$, the dependence is linear and use of eq 3 leads to a fractal dimensionality $d_f \approx 2.3$ for the two cases. Assuming a density $\rho = n/[(4/3)\pi R(n)^{d_f}]$ for the polymer-rich phase, leads to $\rho = 0.61$ and 0.86 for $-k_BT/\epsilon = 2.5$ and 1.0, respectively. These density values compare very well with those predicted from Figure 3 (see curve with symbol △). Thus, equilibrium concentrations are established during the very early stages of SD and the process is completed at $t = 5 \times 10^3\tau$. Further inspection of Figure 5a also reveals that the extent of the linear regime increases with T. In

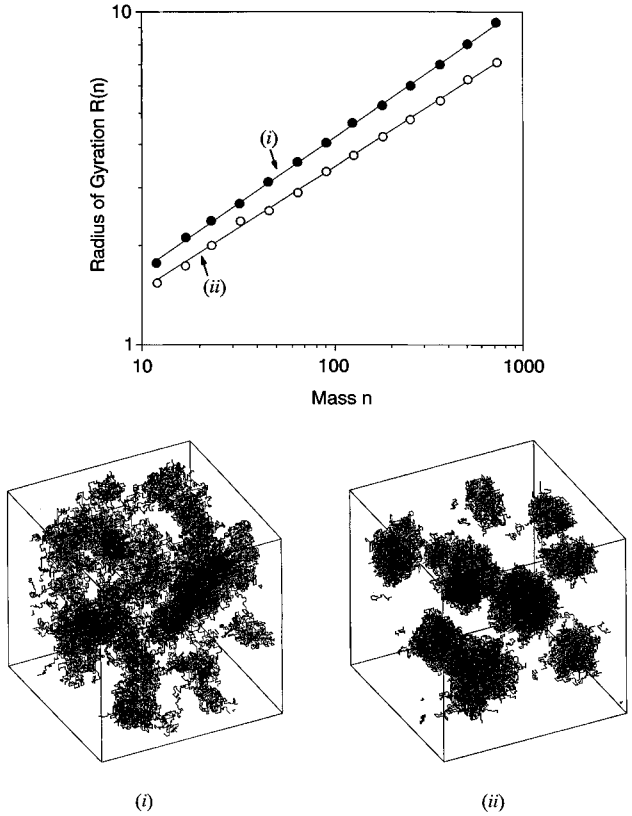

Figure 7. Effect of chain length. The figure is for $N = 10^3$ quenched to $-k_BT/\epsilon = 2.5$ (case i) and for $N = 20$ quenched to $-k_BT/\epsilon = 1.7$ (case ii). For the two cases, we took $V_f = 0.1$ and a simulation time $t \approx 5 \times 10^4\tau$. (a) Radius *vs* size dependence of clusters of polymer segments. (b) Polymer morphologies.

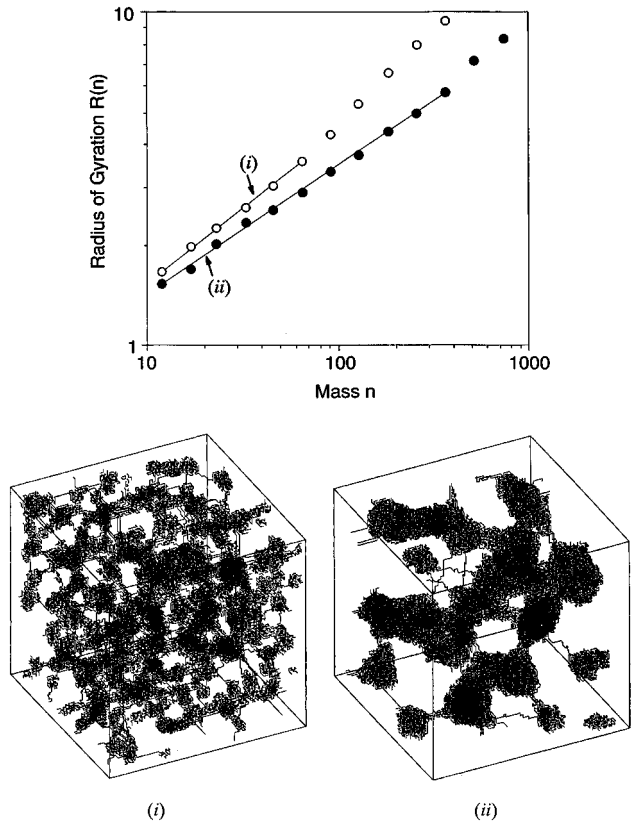

Figure 8. Effect of cooling rate. Case i is for an instantaneous quenching to $-k_BT/\epsilon = 0.5$ and a residence time $\Delta t \approx 5 \times 10^4\tau$; case ii is for a slow and uniform cooling from $-k_BT/\epsilon = 3$ to $-k_BT/\epsilon = 0.5$ within the same time interval Δt. The figure is for $N = 10^3$ and $V_f = 0.1$. (a) Radius *vs* size dependence of clusters of polymer segments. (b) Polymer morphologies.

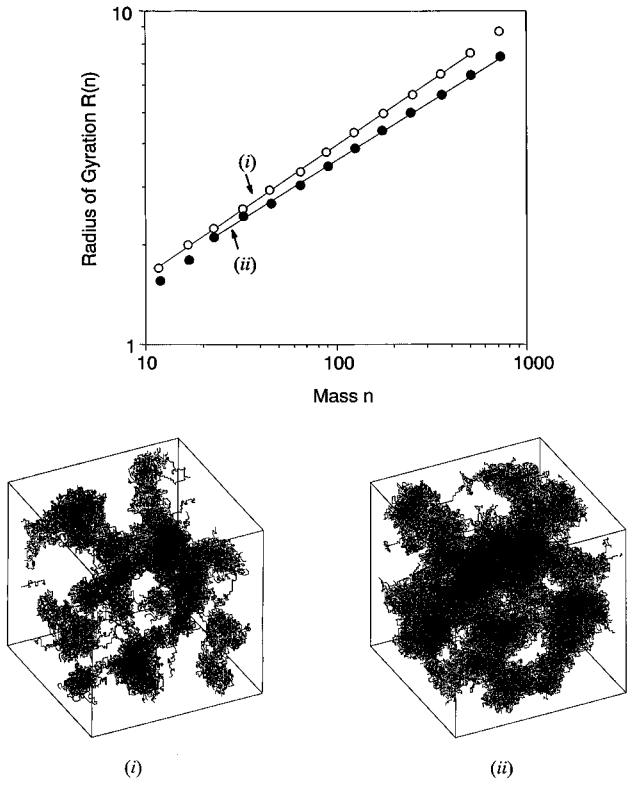

Figure 9. Effect of polymer fraction. The figure is for $N = 10^3$ quenched to $-k_BT/\epsilon = 2.0$ with polymer volume fractions $V_f = 0.1$ (case i) and $V_f = 0.2$ (case ii). The simulation time for the two cases is $t \approx 5 \times 10^4\tau$. (a) Radius vs size dependence of clusters of polymer segments. (b) Polymer morphologies.

other words, the more porous structures obtained at high quenching temperatures are also coarser. This is further illustrated in Figure 5b, which shows the polymer structures obtained at $t = 5 \times 10^3\tau$ for $-k_BT/\epsilon = 2.5$ and 1.0, respectively. A bicontinuous spongelike morphology is observed, in agreement with experimental observation[5,29,30] and with a recent viscoelastic model study.[31] High temperatures are seen to lead to a coarser morphology, whereas lower temperatures form a lacy structure with fine and dense fibrils. The fractal nature of those polymer morphologies is due to the topological constraints created by the connectivity of the segments. We note that a similar situation has been found in the initial droplet growth of quenched Ising systems with medium-range interactions.[32]

We now turn to our model predictions for large simulation times, $t > 10^4\tau$. Inspection of our results for the radius of gyration of solvent domains (right-hand side of Figure 4) reveals that our R_g data can be fitted to

$$R_g^4 = R_{g,0}^4 + K(t - t_0) \qquad (4)$$

in which $R_{g,0}$ and t_0 denote reference values. That new regime occurs at the so-called percolation-to-cluster transition, and eq 4 describes the process of coarsening of solvent domains when the interfaces are not well-defined.[30] Our model predictions (eq 4) for the late stage of SD are in agreement with recent experimental observations on polymer solutions[26] and blends.[24,33,34] Inspection of the right-hand side of Figure 4 also reveals a large increase in rate K with a decrease in quenching temperature. Our model predictions for $R(n)$ *vs* n and polymer morphologies during the coarsening regime are shown in Figure 6 for a quenching time $t = 15 \times 10^4\tau$. Comparing Figures 5b and 6b, we observe a progressive breaking up of the continuous polymer structure into isolated spherical aggregates. Turning to Figure 6a, we also find that these late-stage SD structures have densities very close to those obtained at earlier times, whereas their fractal dimensionalities are higher: $d_f \approx 2.63$.

From our interpretation above, it transpires that the fineness of the structures in Figures 5b and 6b will also be controlled by the relaxation time of the chains, hence by their molecular weight. The effect of chain length is studied in Figure 7 for $t \approx 5 \times 10^4\tau$. Case i is for $N = 10^3$ quenched to $-k_BT/\epsilon = 2.5$; case ii is for $N = 20$ and $-k_BT/\epsilon = 1.7$, which corresponds to a similar quench depth (see Figure 3). From the dependence of $R(n)$ on n (Figure 7a), we observe that the low $N = 20$ (line ii) leads to a denser structure with a higher fractal dimension $d_f = 2.75$, closer to the Euclidean dimension. The structures for the two cases are depicted in Figure 7b. The figure reveals that the detailed fibrillar structure is lost at small N and the polymer is seen to precipitate into dense spherical aggregates. This is the so-called "percolation-to-cluster" transition extensively studied for polymer blends.[24] We note that a similar transition has been obtained in our model with $N = 10^3$ when artificially increasing the mobility of the chains by adding nonlocal reptation moves into the simulations.

The effect of cooling rate for high $N = 10^3$ is studied in Figure 8. Case i is for an instantaneous quenching to $-k_BT/\epsilon = 0.5$ and a residence time $\Delta t \approx 5 \times 10^4\tau$; case ii is for a slow and uniform cooling from $-k_BT/\epsilon = 3$ to $-k_BT/\epsilon = 0.5$ over the same time interval Δt. The dependence of $R(n)$ on n is shown in Figure 8a. The slow cooling (line ii) is seen to lead to a higher fractal dimensionality $d_f \approx 2.65$ (compare with $d_f \approx 2.5$ for line

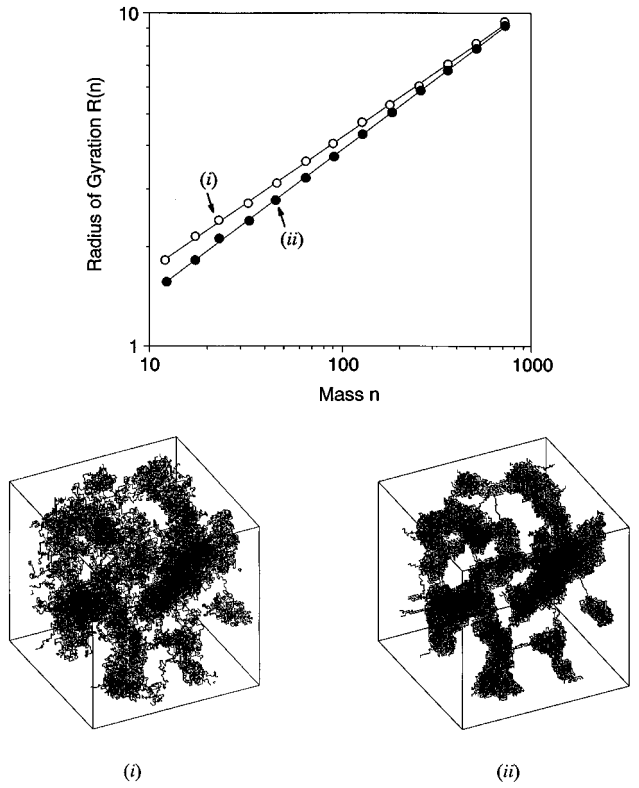

Figure 10. Two-stage quenching. The figure is for $N = 10^3$ and $V_f = 0.1$. Notation is as follows: (i) first stage, quenching at $-k_BT/\epsilon = 2.5$ for a time $t \approx 5 \times 10^4\tau$; (ii) second stage, cooling to $-k_BT/\epsilon = 0.3$ for a time $t \approx 3 \times 10^3\tau$. (a) Radius *vs* size dependence of clusters of polymer segments. (b) Polymer morphologies.

i) and to a wider scaling regime, hence to a coarser structure. This is more clearly exemplified in Figure 6b. We note that the rate effects observed in our model system are in line with those obtained experimentally during thermally-induced phase separation in isotactic polypropylene solutions.[35]

A study of the effect of polymer volume fraction is studied in Figure 9 for $V_f = 0.1$ (case i) and $V_f = 0.2$ (case ii). The figure is for instantaneous quenching to $-k_BT/\epsilon = 2.0$. Figure 9a indicates that the fractal dimensionality increases with V_f: $d_f = 2.59$ for case i, whereas $d_f = 2.8$ for case ii. An estimation of the density $\rho = n/[(4/3)\pi(R^{d_f})^3]$ for the polymer-rich phase leads, in both cases, to $\rho = 0.68$, which is in good agreement with the prediction from the phase diagram of Figure 3. The polymer morphologies for the two cases are depicted in Figure 9b.

Finally, it should be noted that, in several commercial processes, the polymer is quenched in two stages. In flash spinning, for example, a polymer solution under high pressure is first released into a pressure let-down chamber before it is left to exit through the spinnerette. The effect of a two-stage quenching on polymer structure is studied in Figure 10. The chains ($N = 10^3$) were first quenched to $-k_BT/\epsilon = 2.5$ for $t \approx 5 \times 10^4\tau$. This was immediately followed by a deeper cooling to $-k_BT/\epsilon = 0.3$ for a short time $t \approx 3.10^3\tau$. Our data for the dependence of $R(n)$ on n (Figure 10a) reveal that, after the second quenching, the structure densifies and its dimensionality decreases from $d_f = 2.5$ (line i) to $d_f = 2.25$ (line ii). This is more clearly exemplified in Figure 10b, which shows a more compact ribbonlike material at the end of the second stage (case ii).

To conclude, we have presented a mesoscopic model for the development of structure upon quenching of a polymer solution inside a two-phase region. We find that the polymer structure grows in two stages. In the first stage, spinodal decomposition occurs to quickly establish equilibrium concentrations and the sizes of the phase domains increase linearly with time. During that very early stage, the polymer forms a continuous percolated structure whose fine features are exacerbated at very deep quenches. At the percolation-to-cluster transition, the polymer network breaks into isolated aggregates and the sizes grow more slowly as $R^4 \sim Kt$. The polymer structure within that stage coarsens at a rate which increases with quench depth.

References and Notes

(1) Kesting, R. E. *Synthetic Polymeric Membranes*, 2nd ed.; J. Wiley & Sons: New York, 1985.
(2) Dorogy, W. E.; St. Clair, A. K. *J. Appl. Polym. Sci.* **1991**, *43*, 501.
(3) Russel, W. B.; Saville, D. A.; Schowalter, W. R. *Colloidal Dispersions*; Cambridge University: Cambridge, 1989.
(4) Termonia, Y. *Phys. Rev. Lett.* **1994**, *72*, 3678; *J. Polym. Sci., Part B: Polym. Phys.* **1995**, *33*, 279.
(5) Lloyd, D. R.; Kim, S. S.; Kinzer, K. E. *J. Membr. Sci.* **1991**, *64*, 1. Song, S.-W.; Torkelson, J. M. *Macromolecules* **1994**, *27*, 6389.
(6) Eckert, C. A.; Knutson, B. L.; Debenedetti, P. G. *Nature* **1996**, *383*, 313.
(7) de Gennes, P. G. *Scaling Concepts in Polymer Physics*, 3rd printing; Cornell University: Ithaca, NY, 1988. Doi, M.; Edwards, S. F. *The Theory of Polymer Dynamics*: Oxford Science: New York,1989. des Cloiseaux , J.; Jannink, G. *Polymers in Solution*; Clarendon: Oxford, 1990.
(8) Flory, P. J. *J. Chem. Phys.* **1941**, *9*, 660. Huggins, M. L. *J. Chem. Phys.* **1941**, *9*, 440.
(9) Madden, W. G.; Pesci, A. I.; Freed, K. F. *Macromolecules* **1990**, *23*, 1181.
(10) Mackie, A. D.; Panagiotopoulos, A. Z.; Kumar, S. K. *J. Chem. Phys.* **1995**, *102*, 1014.
(11) Byrne, A.; Kiernan, P.; Green, D.; Dawson, K. A. *J. Chem. Phys.* **1995**, *102*, 573.
(12) Ostrovsky, B.; Bar-Yam, Y. *Comput. Polym. Sci.* **1993**, *3*, 9.
(13) Kuznetsov, Y. A.; Timoshenko, E. G.; Dawson, K. A. *J. Chem. Phys.* **1995**, *103*, 4807. Ma, J.; Straub, J. E.; Shakhnovich, E. I. *J. Chem. Phys.* **1995**, *107*, 2615.
(14) Sariban, A.; Binder, K. *Macromolecules* **1991**, *24*, 578.
(15) Termonia, Y.; Smith, P. *Macromolecules* **1988**, *21*, 2184.
(16) Baumgartner, A. *J. Phys. (Paris)* **1982**, *43*, 1407.
(17) Kremer, K.; Baumgartner, A.; Binder, K. *J. Phys. A: Math. Gen.* **1981**, *15*, 2879.
(18) Meirovitch, H.; Lim, H. A. *J. Chem. Phys.* **1990**, *92*, 5144.
(19) Tanaka, G.; Mattice, W. L. *Macromolecules* **1995**, *28*, 1049.
(20) Tanaka, G.; Mattice, W. L. *Macromol. Theory Simul.* **1996**, *5*, 499.
(21) Shinozaki, K.; VanTan, T.; Saito, Y.; Nose, T. *Polymer* **1982**, *23*, 728.
(22) Yan, Q.; Liu, H.; Hu, Y. *Macromolecules* **1996**, *29*, 4066.
(23) That value is obtained as follows. We start by picking a solvent site at random and calculate the radius of the largest sphere that can be centered around that site without overlapping a polymer segment. That process is repeat 1000 times, and R_g is obtained from an average over the 100 largest radius values.
(24) Crist, B. *Macromolecules* **1996**, *29*, 7276.
(25) Siggia, E. D. *Phys. Rev.* **1979**, *A20*, 595.
(26) Lal, J.; Bansil, R. *Macromolecules* **1991**, *24*, 290.
(27) Termonia, Y.; Alexandrowicz, Z. *Phys. Rev. Lett.* **1983**, *51*, 1265.
(28) Termonia, Y. *Phys. Rev. Lett.* **1984**, *53*, 1356.
(29) Aubert, J. H.; Clough, R. L. *Polymer* **1985**, *26*, 2047.
(30) Aubert, J. H. *Macromolecules* **1990**, *23*, 1446.
(31) Taniguchi, T.; Onuki, A. *Phys. Rev. Lett.* **1996**, *77*, 4910.
(32) Heerman, D. W.; Klein, W. *Phys. Rev. Lett.* **1983**, *50*, 1062.
(33) Mirabella, F. M.; Barley, J. S. *J. Polym. Sci., Part B: Polym. Phys.* **1994**, *32*, 2187; **1995**, *33*, 2281.
(34) Crist, B.; Nesarikar, A. R. *Macromolecules* **1995**, *28*, 890.
(35) Lloyd, D. R.; Kim, S. S.; Kinzer, K. E. *J. Membrane Sci.* **1991**, *64*, 1.

MA970565O